Characterization of $GaN_{1-x}As_x$/GaN PN Junction Diodes

H. Qian,[1,a)] K. B. Lee,[1] S. Hosseini Vajargah,[2] S. V. Novikov,[3] I. Guiney,[2] S. Zhang,[2] Z. H. Zaidi,[1] S. Jiang,[1] D. J. Wallis,[2] C. T. Foxon,[3] C. J. Humphreys,[2] and P. A. Houston[1]

[1]*Department of Electronic and Electrical Engineering, University of Sheffield, Sheffield S1 3JD, UK*

[2]*Department of Material Science and Metallurgy, University of Cambridge, Cambridge CB3 0FS, UK*

[3]*School of Physics and Astronomy, University of Nottingham, Nottingham NG7 2RD, UK*

The structural properties and electrical conduction mechanisms of p-type amorphous $GaN_{1-x}As_x$/n-type crystalline GaN PN junction diodes are presented. A hole concentration of 8.5×10^{19} cm^{-3} is achieved which allows a specific contact resistance of 1.3×10^{-4} Ω-cm^2. An increased gallium beam equivalent pressure during growth allows reduced resistivity but can result in the formation of a polycrystalline structure. Temperature dependent current voltage characteristics at low forward bias (<0.35 V) show that conduction is recombination dominated in the amorphous structure whereas a transition from tunneling to recombination is observed in the polycrystalline structure. At higher bias, the currents are space charge limited due to the low carrier density in the n-type region. In reverse bias, tunneling current dominates at low bias (<0.3 V) and becomes recombination dominated at higher reverse bias.

GaN-based PN diodes are attractive for power electronic applications due to the high breakdown field and low power loss and are likely to play an important part in supporting the required large voltages in vertical power devices. However, achieving a high hole concentration (>10^{18} cm^{-3}) remains difficult due to the high activation energy of Mg dopants which can result in high resistivity and poor ohmic contacts. Mg-doped p-type amorphous $GaN_{1-x}As_x$ (0.17<x<0.8) with band gap varying from 0.8-3.4 eV has been demonstrated in an effort to cover a wide range of the solar spectrum for full spectrum solar cells.[1] A hole concentration up to 1×10^{20} cm^{-3} was achieved and the electrical properties of the free carriers were studied.[2] The high hole concentration can be used to improve the performance of electronic devices such as PN diodes, p-GaN gated HFETs and JFETs. However, reports on the characteristics of the material in electronic devices is still lacking. In this paper, for the first time, we present a study of the electrical characteristics of p-$GaN_{1-x}As_x$/n-GaN junction diodes and include the structural properties and transport mechanisms.

[a)] Electronic mail: hqian2@sheffield.ac.uk.

The diode structure is shown in Fig. 1. Firstly, n-GaN templates with a 500 nm n+GaN contact layer with Si concentration of ~5×10^{18} cm^{-3} and 3 μm GaN drift layer with Si concentration of ~2×10^{16} cm^{-3} were grown using metal-organic chemical vapour deposition (MOCVD) on sapphire substrates. Subsequently, 1 μm of Mg-doped $GaN_{1-x}As_x$ was regrown using plasma-assisted molecular beam epitaxy (MBE). Two samples (sample 1 and 2) were grown at different Ga beam equivalent pressures (BEPs) of 2.3×10^{-7} and 2.1×10^{-7} Torr, respectively. These Ga BEPs were chosen to enable growth with the lowest resistivity which, as will be discussed later, is also close to the conditions where transition between amorphous and polycrystalline is possible. The As_2 and Mg BEPs were kept the same at 6.6×10^{-6} and 6×10^{-9} Torr and the substrate temperature was held at 245 ˚C during growth for both samples. In addition, a set of calibration layers were grown to study the dependence of resistivity and contact resistance on Ga BEP which was specified between 1.3×10^{-7} to 2.2×10^{-7} Torr.

The mesa diode was patterned by standard lithography with an active area of 1.2×10^{-3} cm^2 and dry-etched in an inductively coupled plasma system with Cl_2-based gases to access the n+GaN current spreading layer. Ti/Al/Ni/Au and Ni/Au contacts were deposited using a thermal evaporator as the cathode and anode, respectively. It is worth mentioning that most Ni-based ohmic contacts formed on p-GaN in the literature required a post-deposition annealing in O_2 ambient to achieve a good ohmic contact.[3,4] However, in our samples, post-deposition annealing was not required due to the high hole concentration in the p-type material.

Room temperature Hall-effect measurements were carried out with a calibration sample grown on sapphire under the same conditions as sample 1 which showed a hole concentration of 8.5×10^{19} cm^{-3} and a mobility of 0.15 $cm^2V^{-1}s^{-1}$. Circular transmission line model (CTLM) structures were used to study the dependence of specific contact resistance (ρ_c) and resistivity on the Ga BEP. As shown in fig. 2, with Ga BEP increased to 2.2×10^{-7} Torr, ρ_c and resistivity reduce to 1.3×10^{-4} Ω-cm^2 and 0.5 Ω-cm, respectively, which are lower than those typically achieved in p-GaN.[5-8]. However, it is known that an increased Ga BEP can result in the formation of poor quality polycrystalline clusters[2] which is also shown in the transmission electron microscopy (TEM) images in Fig. 3(a). Our approach was to grow at maximum conductivity while avoiding the formation of polycrystalline structure. This is achieved by reducing the Ga BEP to 2.1×10^{-7} Torr. As shown in Fig. 3(b), the growth started with an amorphous layer (~350 nm) followed by a polycrystalline layer which can be identified by the electron diffraction patterns. It is thought that the transition occurred as a result of Ga accumulation on the sample surface during growth.

We were unable to detect any PL or CL signal from amorphous GaNAs layers, similar to what was observed in our previous studies[1,2]. . Energy dispersive x-ray spectroscopy (EDS) analysis was carried out on sample 2 to determine the

average composition of each region. As shown in Fig. 3 (c) and 3 (d), $GaN_{0.34}As_{0.66}$ and $GaN_{0.21}As_{0.79}$ in mole fractions were measured in the polycrystalline and amorphous regions, respectively. The corresponding band gap energies ~1 eV are estimated according to the band anti-crossing model and previously published results,[1] The room temperature turn-on voltages (defined at 10 mA/cm^2) for sample 1 and 2 are 1.29 and 1.07 V, respectively, which fall within the predicted band gap range.

Fig. 4(a) and 4(b) show the temperature dependent current-voltage (I-V-T) characteristics for sample 1 and 2 measured over the temperature range of 305 – 430 K on a semi-log scale. The forward currents increase exponentially at low bias (<0.35V) and non-exponentially at higher bias voltage. In order to identify the dominant current conduction mechanism at low bias regime, the reverse saturation current I_0 and ideality factor n is extracted by fitting to the Shockley model described by:[9]

$$I = I_0\left[exp\left[\frac{q(V-IR_S)}{nkT}\right] - 1\right] \quad (1)$$

where R_s is the series resistance, k the Boltzmann constant and T the temperature. In the classical generation-recombination (G-R) model, n lies between 1-2 and is independent of temperature and I_0 is characterized by:

$$I_0 \propto \exp\left[-\frac{E_{ac}}{2kT}\right] \quad (2)$$

where E_{ac} is the activation energy that describes the energy of the recombination centre.

Good curve fitting was obtained at the low bias regime (<0.35V) where series resistance and high injection effect are insignificant. The room temperature ideality factors extracted from sample 1 and sample 2 are 4.3 and 3.5, respectively. Several groups have reported ideality factors greater than two in GaN PN junctions[8,10,11] which contradicts the G-R model. The exact reason for the high ideality factor in our samples is unclear. Shah et al. attributed this behavior to the summation of n of each rectifying junction within the structure, including the contacts[10]. In our case, although the contacts are ohmic as confirmed by CTLM measurements, at low currents the n+/n-GaN junction might contribute to additional n due to the abrupt change in doping profile. Another possibility, as explained by Hurni et al., is due to the high density of interfacial defects, dislocation and non-uniformity of the doping.[8] On the other hand, a tunneling current in the junction may also result in $n>2$ which can be identified when n is inversely proportional to T.[11-14]

The plot of n versus T is given in Fig. 5. In sample 1, n reduces to 3.8 when T increases to 340 K which is a signature of a tunneling mechanism. Fig. 6 shows the temperature dependence of I_0. As shown in the inset, $\ln(I_0)$ is observed to be proportional to T at temperatures below 340 K which can be described by a multi-step tunneling mechanism similar to

amorphous silicon PN junctions[12] and GaN LEDs[15]. As a polycrystalline structure, tunneling is expected at the grain boundaries between the crystallites.[16] In addition, the high density of defects within the crystallites, as revealed by the TEM analysis, may also act mid-gap states and lead to defect-assisted tunneling. Above 340 K, n becomes independent of T indicating a possible transition to the G-R mechanism. However, a non-linear fit was observed from the Arrhenius plot (Fig. 6) whereas one would expect a straight line in the case of recombination dominated conduction. A similar non-linearity has been observed in poly-Silicon PN diodes[16] where two activation energies were obtained, indicating the presence of two energy levels within the band gap. In our case, the activation energy gradually increases from 0.32 to 0.48 eV as the temperature increases, which may indicate multiple energy levels distributed within the band gap. It is speculated that the recombination process occurs at the lower energy tunneling sites at low temperature and, as temperature increases, higher energy levels are involved which moves the activation energy towards higher values. In sample 2, on the other hand, n remains almost constant throughout the temperature range. $\ln(I_0)$ is observed to have a linear dependence on $1/kT$ which is consistent with eq. 2. E_{ac} = 0.56 eV is extracted from Arrhenius plot which is in agreement with the half band gap value of $GaN_{0.21}As_{0.79}$. This is evidence that recombination in the amorphous $GaN_{0.21}As_{0.79}$ part of the depletion region dominates the conduction.

Fig. 7 shows the forward current characteristics on a log-log scale. At the higher bias (>0.35 V), the currents follow a power law (V^m) dependence in both samples. The value of m is greater than two which indicates that the current is space charge limited.[14] This is understandable as the electron concentration of the drift layer is more than three orders of magnitude lower than the hole concentration in the p-type region, and a space charge limited region forms at high current injection levels. The reduced m at higher bias indicates the conduction is moving towards series resistance limited.

The temperature dependent reverse currents are plotted against reverse voltage on a log-log scale as shown in Fig. 8. Two distinctive regions can be seen in both samples. At $V_r > 0.3$ V (except T < 340 K regime in sample 1), the reverse currents follow a $V^{0.5}$ dependence which is known to be the generation current within the depletion region.[14] The Arrhenius plots of the reverse currents at 0.5 V yield activation energies of 0.28 to 0.37 eV for sample 1 and 0.52 eV for sample 2. The increase of activation energy of sample 1 is believed to be due to a similar behavior as in the low forward bias regime which involves multiple energy levels. At $V_r < 0.3$ V, the reverse currents do not follow the $V^{0.5}$ relationship but are found to have a similar T dependence as in the multi-step tunneling case. Additionally, a similar trend is observed in sample 1 for all applied voltages at $T < 340$ K. This behavior coincides with the transition from tunneling to recombination under forward bias in sample 1.

In summary, we have studied the structural and electrical characteristics of $GaN_{1-x}As_x$/GaN PN diodes. The material transits from amorphous into polycrystalline with increased Ga BEP. The formation of an amorphous layer with low resistivity requires careful control of the Ga BEP during growth. At low forward bias, recombination dominates in the amorphous structure whereas a transition from tunneling to recombination is observed in the polycrystalline structure which reveals the existence of multiple defect levels. At high forward bias, the currents are space charge limited due the low carrier density in the n-type region. In reverse bias, tunneling current dominates at low voltage and becomes recombination dominated at higher bias. The high hole concentration is beneficial for good ohmic contacts and shows promise for low-loss GaN-based power diodes and JFETs. Practical diodes designed to withstand high reverse breakdown voltage will likely require homogeneous amorphous growth with less As incorporation in order to increase the band gap so that the carrier generation and tunneling are limited.

Acknowledgement: This work was undertaken with support from the EPSRC (EP/K014471/1). The authors would like to acknowledge Prof. K.M. Yu and Prof. W. Walukiewicz for discussions.

[1]S. V. Novikov, C. R.Staddon, C. T.Foxon, K. M.Yu, R. Broesler, M. Hawkridge, Z. Liliental-Weber, J. Denlinger, I. Demchenko, F. Luckert, P. R. Edwards, R. W. Martin, W. Walukiewicz, Journal of Crystal Growth 323 (2011) 60–63
[2]A. X. Levander, S. V. Novikov, Z. Liliental-Weber, R. dos Reis, O. D. Dubon, J. Wu, C. T. Foxon, K. M. Yu, and W. Walukiewicz, Journal of Applied Physics 110, 093702 (2011)
[3]J. -K. Ho, C. -S. Jong, C. -C. Chiu, C. -N. Huang, K. -K. Shih, L. -C. Chen, F. -R. Chen, and J. -J. Kai, Journal of Applied Physics 86, 4491 (1999)
[4]X. J. Li, D. G. Zhao, D. S. Jiang, Z. S. Liu, P. Chen, J. J. Zhu, L. C. Le, J. Yang, X. G. He, S. M. Zhang, B. S. Zhang, J. P. Liu, and H. Yang, Journal of Applied Physics 116, 163708 (2014)
[5]J. -D. Hwang, Z. -Y. Lai, C. -Y. Wu and S. -J. Chang, Japanese Journal of Applied Physics, Vol. 44, No. 4A, (2005), pp. 1726–1729
[6]M. Scherer, V. Schwegler, M. Seyboth, C. Kirchner, M. Kamp, A. Pelzmann, and M. Drechsler, Journal of Applied Physics 89, 8339 (2001)
[7]A. Dussaigne, B. Damilano, J. Brault, J. Massies, E. Feltin, and N. Grandjean, Journal of Applied Physics 103, 013110 (2008)
[8]C. A. Hurni, J. R. Lang, P. G. Burke, and J. S. Speck, Applied Physics Letters 101, 102106 (2012)
[9]C. T. Sah, R. N. Noyce, and W. Shockley, Proc. IRE 45, 1228 (1957)
[10]J. M. Shah, Y. -L. Li, Th. Gessmann, and E. F. Schubert, Journal of Applied Physics Vol. 94, No. 4, (2003)
[11]J. B. Fedison, T. P. Chow, H. Lu, and I. B. Bhat, Applied Physics Letters, Vol. 72, No. 22, (1998)
[12]A. J. Harris, R. S. Walker, and R. Sneddon, Journal of Applied Physics 51, 4287 (1980)
[13]H. Matsuura, T. Okuno, H. Okushi, and K. Tanaka, Journal of Applied Physics 55, 1012 (1984)
[14]H. Mimura and Y. Hatanaka, Journal of Applied Physics 71, 2315 (1992)
[15]Q. Shan, D. S. Meyaard, Q. Dai, J. Cho, E. F. Schubert, J. K. Son, and C. Sone, Applied Physics Letters 99, 253506 (2011)
[16]M. Dutoit and F. Sollberger, J. Electrochem. Soc.: Solid-State Science And Technology, Vol. 125, No. 10, 1648 (1978)

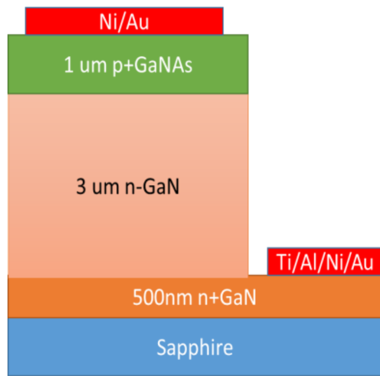

Fig. 1. Device structure of GaN/ $GaN_{1-X}As_X$ PN junction diode.

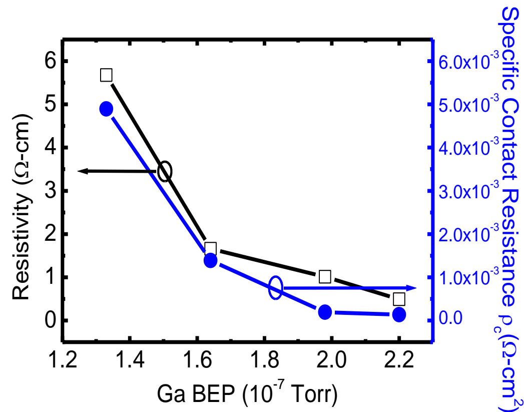

Fig. 2. Dependence of GaNAs resistivity (black) and specific contact resistance (blue) on Ga flux during growth.

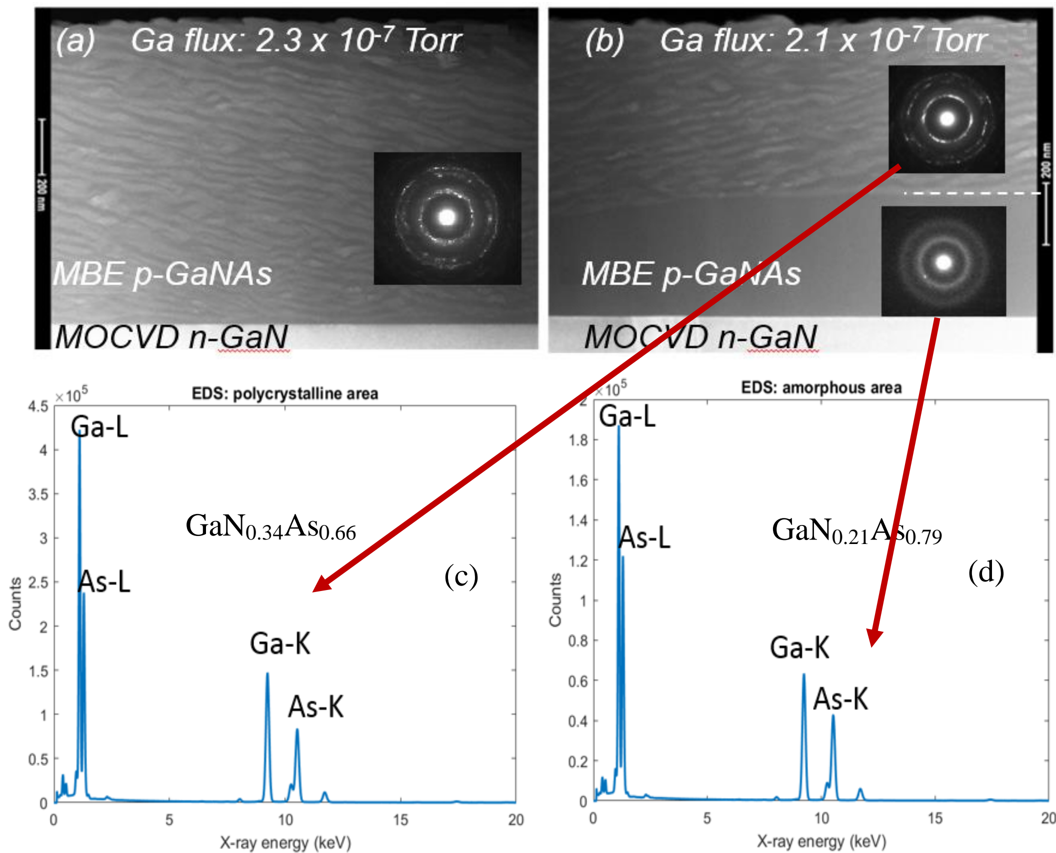

Fig. 3. TEM images with electron diffraction patterns of GaNAs layers showing (a) sample 1 (all-polycrystalline structure), and (b) sample 2 (amorphous/polycrystalline structure); EDS results showing the composition of (c) polycrystalline region, and (d) amorphous region.

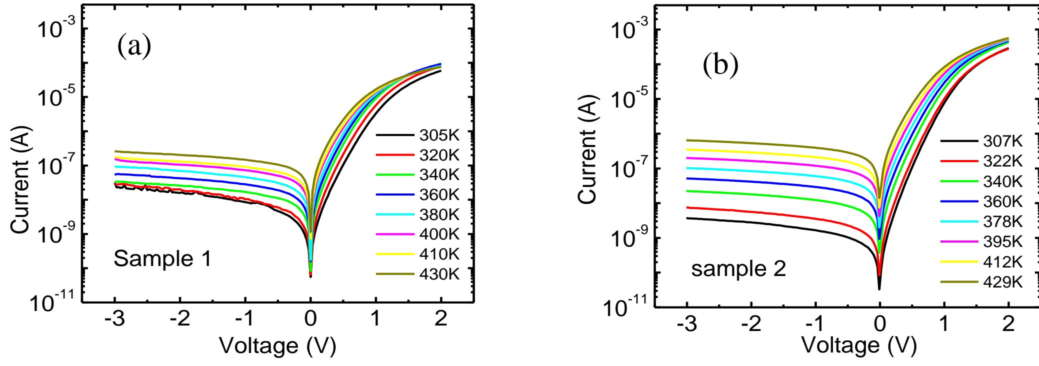

Fig.4. Temperature dependent IV characteristics on semi-log scale of (a) sample 1, and (b) sample 2.

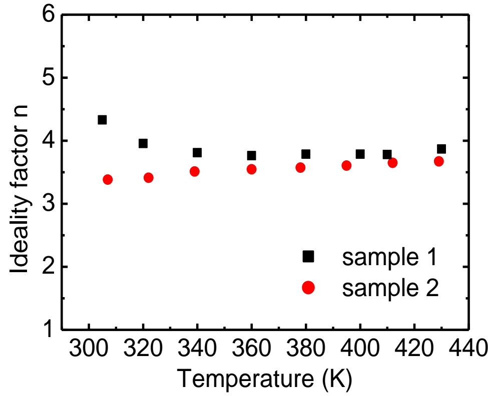

Fig.5. Temperature dependent of ideality factor n

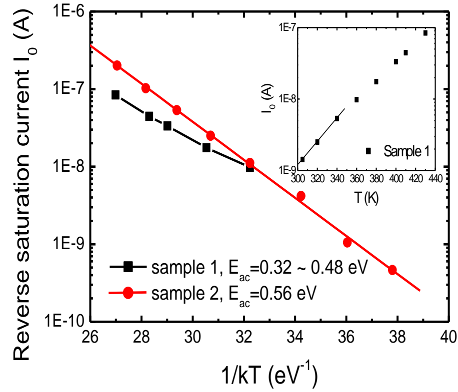

Fig.6. Temperature dependence of I_0 as a function of $1/kT$; Inset: I_0 as a function of T of sample 1. I_0 is proportional to T below 340 K indicating a multi-step tunneling mechanism.

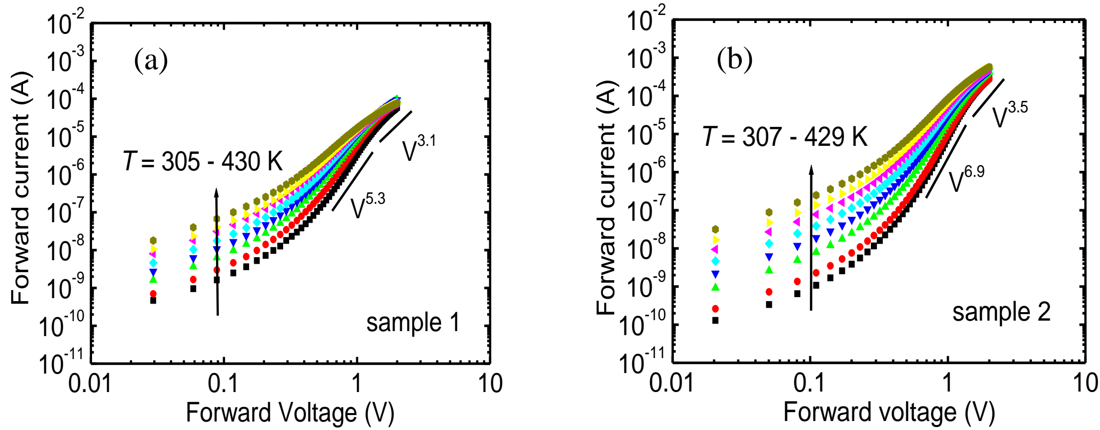

Fig.7. Forward current characteristics on a log-log scale of (a) sample 1, and (b) sample 2.

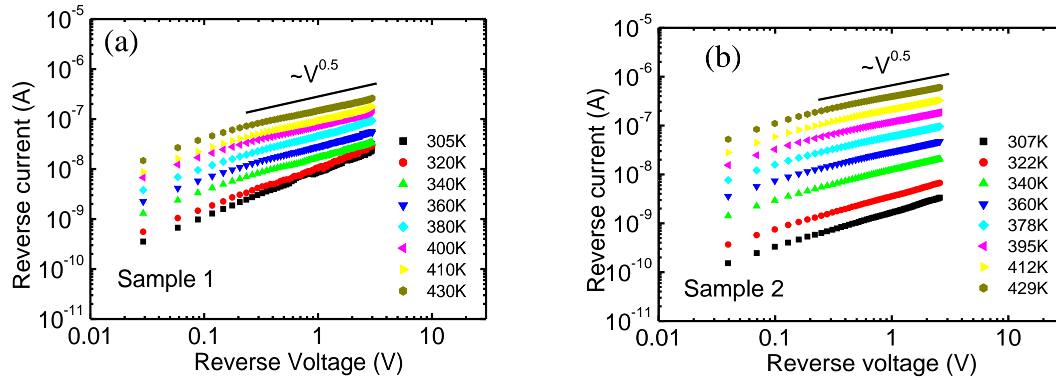

Fig.8. Reverse current characteristics on a log-log scale of (a) sample 1, and (b) sample 2.

Fig. 1. Device structure of $GaN_{1-X}As_x$/GaN PN junction diode.

Fig. 2. Dependence of GaNAs resistivity (black) and specific contact resistance (blue) on Ga flux during growth.

Fig. 3. TEM images with electron diffraction patterns of GaNAs layers showing (a) sample 1 (all-polycrystalline structure), and (b) sample 2 (amorphous/polycrystalline structure); EDS results showing the composition of (c) polycrystalline region, and (d) amorphous region.

Fig. 4. Temperature dependent IV characteristics on a semi-log scale of (a) sample 1, and (b) sample 2.

Fig. 5. Temperature dependence of ideality factor n.

Fig.6. Temperature dependence of I0 as a function of 1/kT; Inset: I0 as a function of T of sample 1. I0 is proportional to T below 340 K indicating a multi-step tunneling mechanism.

Fig. 7. Forward current characteristics on a log-log scale of (a) sample 1, and (b) sample 2.

Fig. 8. Reverse current characteristics on a log-log scale of (a) sample 1, and (b) sample 2.